

Supporting Information

Weaving colloidal webs around droplets – Spontaneous assembly of extended colloidal networks encasing microfluidic droplet ensembles

Lu Zheng[♀], Leon Yoon Ho[♀] and Saif A. Khan^{♀}*

[♀]Department of Chemical and Biomolecular Engineering, 4 Engineering Drive 4, National
University of Singapore, Singapore 117585, Singapore

*Corresponding Author. Email: saifkhan@nus.edu.sg

Detailed Methods

Oil-in-water (O/W) emulsion generation using capillary microfluidic emulsion generator

O/W emulsions were generated using a glass capillary microfluidic setup (A schematic of the experimental setup is provided in Figure S1). The axisymmetric coaxial glass capillary flow-focusing device was assembled using a square and round capillary, as demonstrated by our group previously.^{1,2} The surface of round capillary was hydrophilized with the treatment of oxygen plasma (100 W) for 120 s. The aqueous continuous phase (W) used was a 1.5 wt% PVA aqueous solution. The dispersed phase (O) was one of the following two: (i) DCM, (ii) ROY in DCM (250 mg/mL). W and O phases were infused from the two ends of the square capillary through the outer coaxial region using syringe pumps (Harvard PHD 22/2000 series) at flow rates of 80 and 40 $\mu\text{L}/\text{min}$ respectively. The fluids were hydrodynamically flow focused through the nozzle of the round capillary resulting in the formation of the emulsion droplets. (Figure S1b, S1c)

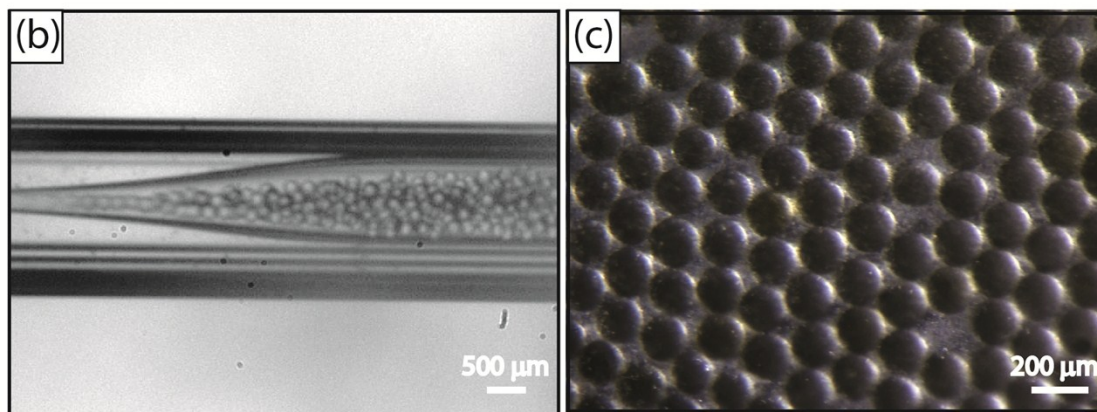
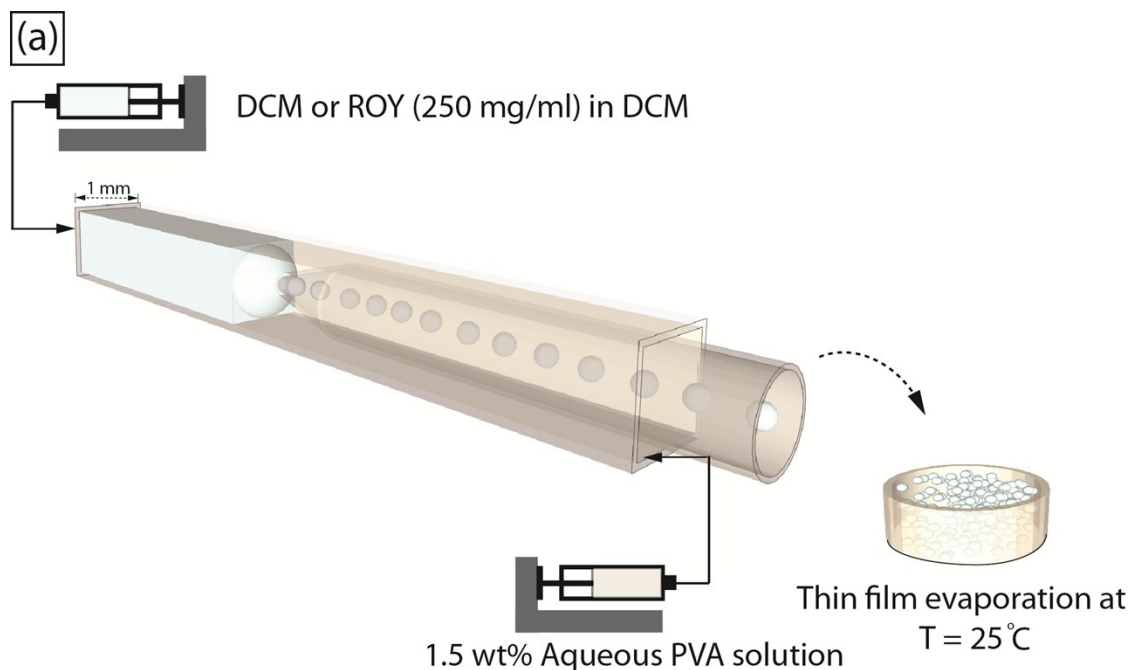


Figure S1: Schematic of experimental setup. Emulsion generation is performed in a concentric microfluidic glass capillary setup, where a square capillary (I.D. = 1 mm) houses a tapered round capillary (O.D. = 1 mm). The two ends of the square capillary function as inlets and the round capillary functions as a collection tube and outlet. The continuous phase (CP) of water (with dissolved surfactants) and a dispersed phase (DP) of DCM (or ROY in DCM) solution are infused by syringe pumps into the square capillary. The emulsions are collected into a glass well (5.1 cm ID), containing a 2 mm film of β -cyclodextrin aqueous solution.

Harvesting of DCM- β -cyclodextrin IC Crystals

Due to the transient nature of the IC colloidal crystal network formation process, it is not feasible to harvest the IC crystals directly from the glass well. As an alternative, we represent the IC crystal aggregates/network formation process by providing an interface of DCM and 1 wt% β -cyclodextrin aqueous solution in a GC vial. 600 μ L of DCM was pipetted into the GC vial first, due to its higher density (1.325 g/mL at 25°C as specified on safety data sheet of Sigma-Aldrich) than water, followed by careful addition of another 600 μ L of 1 wt% β -cyclodextrin aqueous solution on top. Immediate cloudiness was observed both at the interface and inside the aqueous phase, in decreasing intensity. The GC vial was then sealed and kept for 7 days to allow more IC crystals to form through diffusion of DCM. Finally, a thick solid white layer was formed at the interface and harvested for further characterization. (Figure S2)

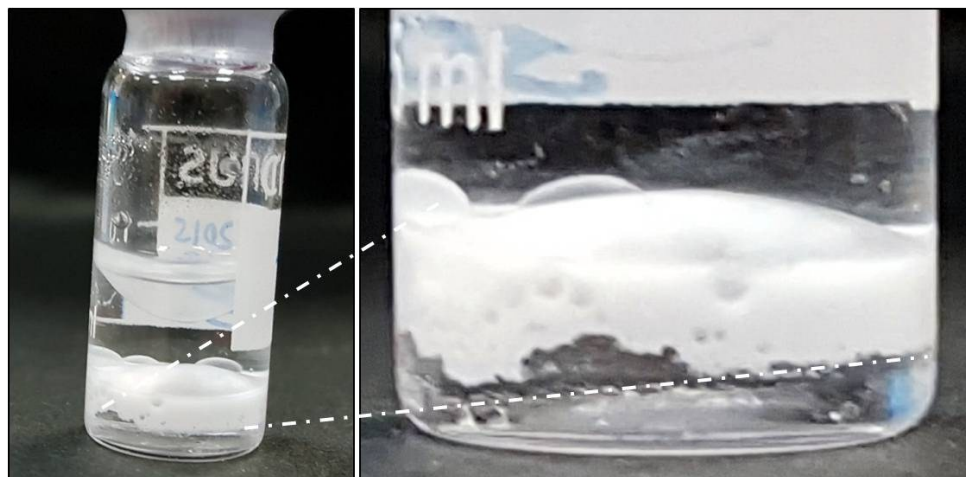


Figure S2: Optical image of colloidal crystal aggregates formed at the interface of DCM and 1 wt% β -cyclodextrin aqueous solution.

Model for Diffusion from a Hexagonally Patterned Planar Array of Point Sources

A simple diffusion-driven mass transfer model was solved to understand the system behavior. Briefly, each droplet was treated as a point source continuously releasing DCM at a time-dependent rate. To estimate the latter, we used the shrinkage rate of ROY-containing DCM droplets (see below). We employed the well-known analytical solution for time-dependent diffusive transport from a continuous point source in three dimensions³ (see Equation 1 below), and applied it to a hexagonally-patterned planar array of point sources ('droplets'), with a characteristic spacing equivalent to the inter-droplet spacing in the actual experimental situation. The linearity of Equation 1 allows for a simple additive contribution from all the point sources in the array to the DCM concentration at any location in the ensemble. The array used to calculate the 2-D concentration maps in Figure 2(a)-(c) was composed from a limited number (19) of point sources, roughly equivalent to two close-packed droplet 'shells' around a central droplet, in order to keep the calculations tractable, whilst yielding qualitatively accurate results.

$$C(r,t) = \frac{1}{8(\pi D)^{\frac{3}{2}}} \int_0^t \frac{e^{-\frac{r^2}{4D(t-t')}}}{(t-t')^{\frac{3}{2}}} \dot{m}(t') dt' \quad \text{(Eqn. 1)}$$

Where

$C(r,t)$ is the concentration of the solute at a distance r from the point source at current time t , mol/m³;

$\dot{m}(t')$ is the time-dependent release rate at the point source, mol/s;

D is diffusion coefficient of the solute in the medium, m²/s;

t is a parameter for current time, s;

Shrinkage Rate Measurement of Emulsion Droplets

Shrinkage of ROY droplets surrounded by IC networks was measured over time and plotted, as shown in Figure S3. Toldy *et al.*⁴ reported a linear fit to estimate shrinkage rates in such systems; we followed this method, and estimated a shrinkage rate of $\sim 0.019 \mu\text{m/s}$. Shrinkage of ROY-DCM droplets in ultra pure water (without formation of IC networks) was also measured and shrinkage rate was found to be $\sim 0.026 \mu\text{m/s}$, which is faster than the case with IC networks. The slower shrinkage rate in the presence of IC networks could be due to two primary reasons: the IC layer might slow down the diffusion of DCM, and a second more subtle reason could be the crowding of droplets when the IC network holds them in place, which locally raises the DCM concentration, thus decreasing the gradient for outward diffusion. We couldn't measure shrinkage rate of DCM droplets without ROY, due to the cloudy CD network around the droplets.

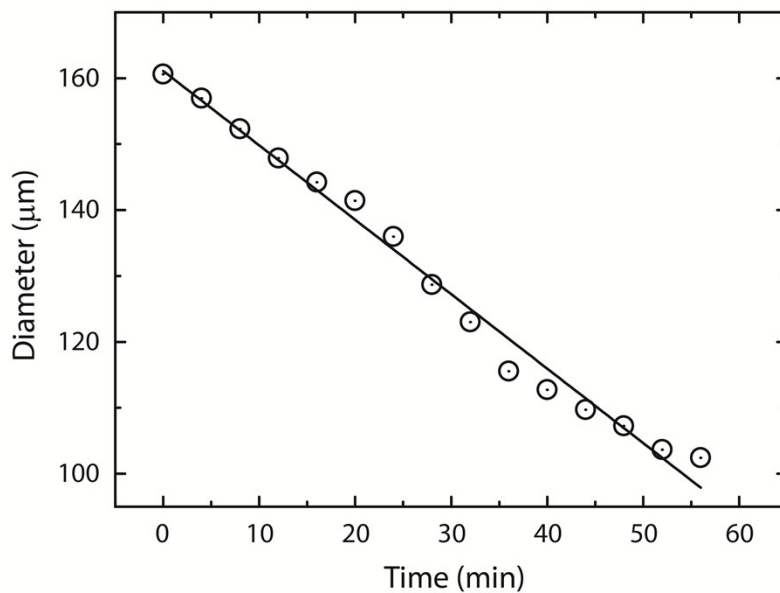


Figure S3: Droplet size measurements over time, measured for shrinking ROY droplets surrounded by dynamic IC networks.

Control Experiment of Evaporative Crystallization without Colloidal Crystal Network

A control experiment was conducted to confirm the effectiveness of the colloidal crystal network for emulsion-based evaporative crystallization of ROY. Droplets containing ROY in DCM (250 mg/ml) solution were generated by the same method mentioned above. Instead of collecting the emulsions into a 2 mm film of β -cyclodextrin aqueous solution, ultra pure water was used as the collection film. In the control experiment, both coalescence of droplets and severe secondary nucleation were observed (Figure S4).

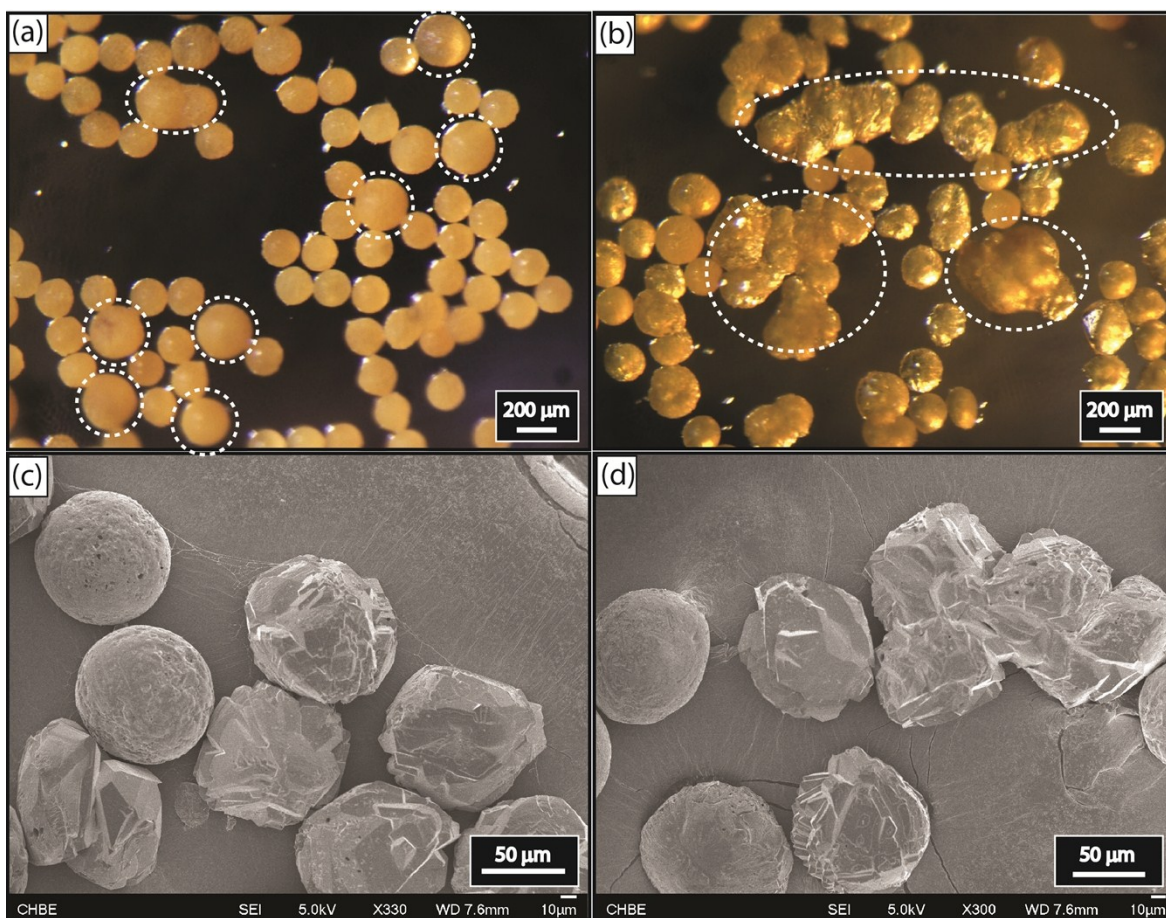


Figure S4. Optical [(a), (b)] and FESEM [(c), (d)] images of pure ROY (250 mg/mL) both coalescence (S4a) and secondary nucleation (S4b) were observed and affected final product quality.

DSC Characterization of ROY

DSC analysis was performed to find the polymorphism of obtained ROY SAs. DSC thermograms were recorded at 3 °C/min from 70 to 130°C, corresponding to the melting range of ROY forms⁵ (Figure S5). It was found that a majority of Y polymorph of ROY was obtained with a minority of OP polymorph.

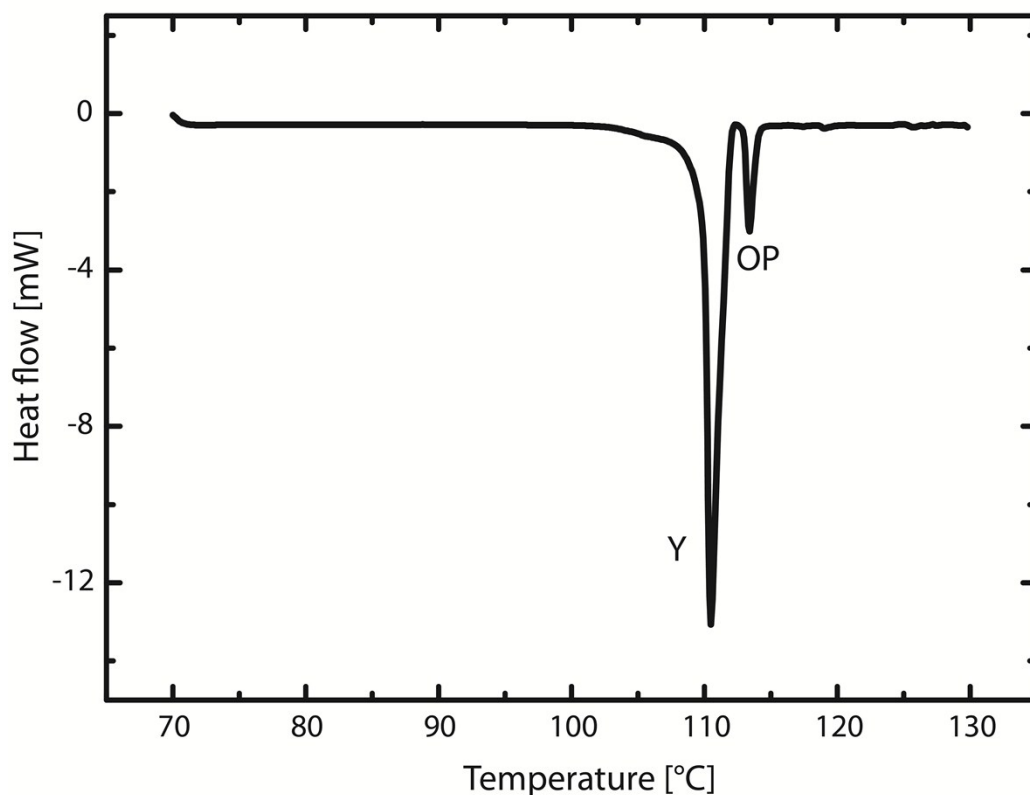


Figure S5: Differential scanning calorimetry (DSC) profile for ROY SAs obtained. Characteristic exotherms for Y and OP polymorphs of ROY are found at 110 °C and 113 °C respectively.⁵

References

- 1 A. I. Toldy, A. Z. M. Badruddoza, L. Zheng, T. A. Hatton, R. Gunawan, R. Rajagopalan, *et al.*, *Cryst. Growth Des.*, 2012, **12**, 3977-3982.
- 2 R. A. L. Leon, A. Z. M. Badruddoza, L. Zheng, E. W. Q. Yeap, A. I. Toldy, K. Y. Wong, *et al.*, *Cryst. Growth Des.*, 2015, **15**, 212-218.
- 3 W. M. Deen, *Analysis of Transport Phenomena*. New York: Oxford University Press, 1998.
- 4 A. I. Toldy, L. Zheng, A. Z. M. Badruddoza, T. A. Hatton, and S. A. Khan, *Cryst. Growth Des.*, 2014, **14**, 3485-3492.
- 5 L. Yu, *Acc. Chem. Res.*, 2010, **43**, 1257-1266.